Materials Physics and Mechanics 47 (2021) 306-314 Received: February 24, 2021

STRUCTURAL AND MAGNETIC PROPERTIES OF ZINC DOPED COPPER FERRITE SYNTHESIZED BY SOL-GEL AND HYDROTHERMAL ROUTE

Naveen Kumar, Deepak Singh, Abhishek Nigam*, Omprakash Rajpoot, Mayank Kumar Yadav, Yogendra Pratap Singh, P. Shakti Prakash, Samarjit Singh

Applied Mechanics Department, Motilal Nehru National Institute of Technology Allahabad, Prayagraj-211004, India

*e-mail: abhishek.bmi5@gmail.com

Abstract. In this work, Cu-Zn spinel ferrites having chemical formula $Cu_{(1-x)}Zn_xFe_2O_4$ for x ranging from 0.2 to 0.8 were synthesized by sol-gel auto-combustion method and hydrothermal method with a step size of 0.2. The effect of Zn doping on structural properties, crystallite size, and magnetic properties synthesized by both methods are reported. Rietveld refinement of the XRD patterns was analyzed using Maud for the determination of crystallite size. The X-ray diffraction pattern shows that single phase Cu-Zn spinel ferrite was formed, and it has a cubic structure. Additionally, the lattice parameter size increases with Zn doping and then decreases after x=0.6. A vibrating sample magnetometer (VSM) was done to determine magnetic properties like saturation magnetization (Ms), remanence (Mr), and coercivity (Hc). The scanning electron microscopy (SEM) shows the morphology and confirms the average particle size.

Keywords: copper, hydrothermal, sol-gel, spinel ferrite, zinc

1. Introduction

Ferrites are ceramic materials possessing properties like very high electrical resistivity, low power loss at high frequencies, suitable for temporary and permanent magnetic applications due to their spontaneous magnetization and conductivity behavior like those of semiconductors [1,2]. Ferrites with narrow hysteresis loop form softs magnets, which are used for audio transformers, television transformers, gyrators, inductance cores. Ferrite nanoparticles have high electrical resistivity because they have a better response at high frequencies [3,4]. Ferrites are the outstanding core material choice for frequencies from 10 kHz to a few MHz, when we require low cost, high stability, and lowest volume [5,6]. Ferrites are widely studied due to their applications in protecting living bodies from microwaves, anechoic chamber, satellite communication, microwave darkroom, and microwave industries as radar absorbing material. Ferrites having chemical formula MFe_2O_4 with the spinel structure have face-centered cubic (FCC) lattice of the oxygen ions. Every spinel unit cell comprises eight formula units. In every unit cell, there exists 64 tetrahedral sites and 32 octahedral sites. Therefore, their composition depends on the structural, chemical, and electromagnetic properties of ferrites, dependent on the preparation methodologies [7,8]. Zn doped Cu ferrites have a significant temperature-dependent magnetic moment near body temperature, therefore successfully used in temperature sensor in MRI properties [9-11]. Various cations can be placed at these tetrahedral sites and octahedral sites to get interesting

http://dx.doi.org/10.18149/MPM.4722021_12

chemical and physical [12,13]. It is reported that Ni–Cu–Zn ferrites with less content of Zn could obtain high Curie temperature, but the initial permeability of Ni–Cu–Zn ferrites reached only up to 2000 [14-16]. This paper will distinguish two well-known methods of preparation ferrite nano powders to synthesize Cu-Zn spinel ferrites. The study's objective was to investigate the effect of Zn substitution on magnetic (saturation magnetization, remanence, and coercivity) and structural properties (lattice parameter, grain size, and crystallite size). The prepared ferrite nano powders are characterized by using X-ray diffraction (XRD), vibrating-sample magnetometer (VSM), and scanning electron microscopy (SEM).

2. Experimentation

Methodology. Cu-Zn spinel was synthesized by using the sol-gel auto combustion method and hydrothermal method. A balanced equation for synthesis by each method is mentioned below:

$$(1-x)Cu(NO_3)_2.3H_2O + x(CH_3COO)_2Zn.2H_2O + 2Fe(NO_3)_2.9H_2O + 3C_6H_8O_7.H_2O = Cu_{(1-x)}Zn_xFe_2O_4. \quad (1)$$

Synthesis by Sol-gel Route. Stoichiometric calculations were done for the synthesis of $Cu_{(1-x)}Zn_xFe_2O_4$. Copper nitrate ($Cu(NO_3)_2.3H_2O$), Zinc acetate ($(CH_3COO)_2Zn.2H_2O$), Iron nitrate ($Fe(NO_3)_3.9H_2O$), and citric acid were used as precursors. All nitrates and citric acid were dissolved insufficient amount of distilled water to form a clear solution to obtain metal ions solution in separate beakers. All the nitrates were mixed in a beaker and were kept for continuous stirring for 15 minutes, as shown in Fig. 1. Citric acid was added to the solution as a chelating agent, and then ammonia solution was slowly added to maintain the pH of the solution at 7 with continuous stirring. Citric acid to metal ion ratio was taken as 1:1 [4]. The temperature of the hotplate was gradually increased to 60ºC. Then the solution was heated and stirred for about 4 hours. The gel was formed after 4 hours, and it was heated at the same temperature for about 25 minutes. Auto combustion took place, and a homogenous powder was formed. Various gases were evolved during this process. After complete combustion of the sample, the hotplate temperature was decreased slowly. The product of auto combustion was grounded into a fine powder with the help of agate mortar. The powder formed was calcinated at 750 ºC for 8 hours to form crystalline spinel ferrite. The phase identification of the calcined powder was performed by X-ray diffraction (XRD) using Cu-Kα radiation. Magnetic properties of the spinel ferrite like saturation magnetic flux, remnant magnetic flux, and coercive force were determined using VSM.

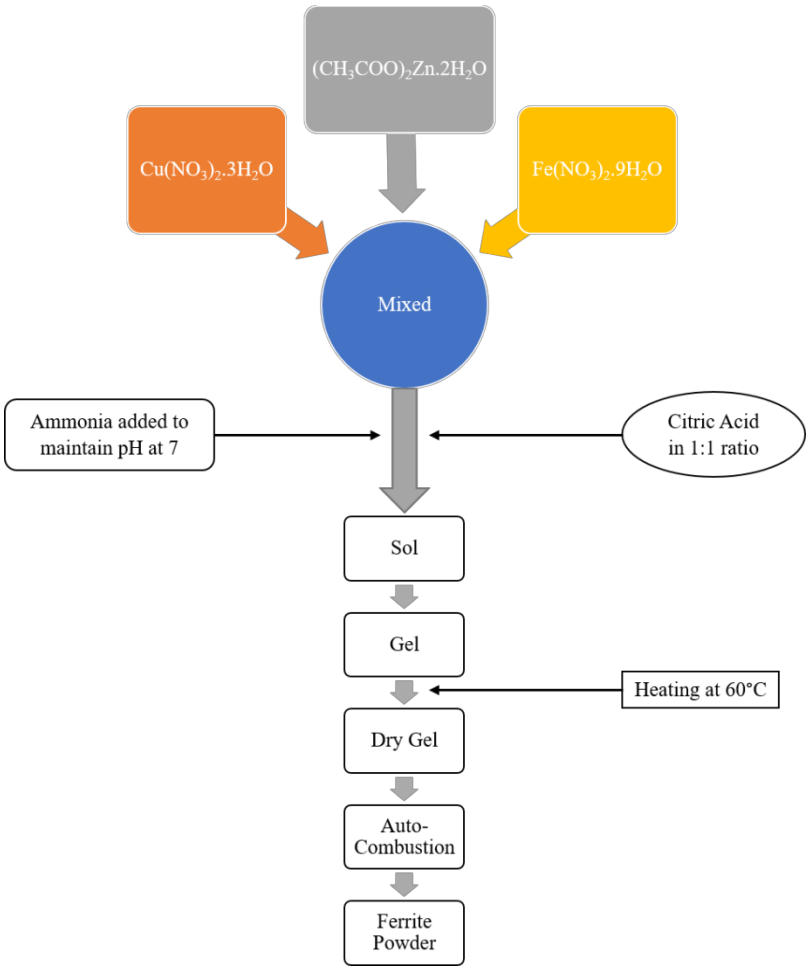

Fig. 1. Typical flow chart of Sol-Gel method for synthesizing Cu-Zn spinel ferrite

Synthesis by Hydrothermal Route. Stoichiometric calculations were done for the synthesis of $Cu_{(1-x)}Zn_xFe_2O_4$. Copper nitrate ($Cu(NO_3)_2.3H_2O$), Zinc acetate ($(CH_3COO)_2Zn.2H_2O$), and Iron nitrate ($Fe(NO_3)_3.9H_2O$) were used as precursors. All nitrates dissolved an insufficient amount of distilled water to form a clear solution to obtain metal ions solution in separate beakers, as shown in Fig. 2. The 2M NaOH solution was prepared by adding 16 gm NaOH in 200 mL of distilled water to maintain the pH of 12.5. A beaker with iron nitrate solution was placed on the hotplate, and a magnetic capsule (stirrer) was put in the solution. Copper nitrate and zinc acetate solution were added to it under continuous stirring. 2M NaOH solution was slowly added to the solution to maintain the pH of the solution at 12.5 with continuous stirring. The temperature of the hotplate was kept at room temperature. Then the solution was stirred for about 2 hours for complete mixing of the metal ions. The solution was poured into a Teflon tube and kept at 220 ºC for 8 hours in the oven. The precipitate was formed after 8 hours of heating; this precipitate was filtered using filter paper and distilled water. After filtering the precipitate, it was again kept in the oven for 24 hours at 60ºC for drying along with filter paper. With the help of a spatula, powder formed after drying was collected from filter paper and grounded to a fine powder using agate mortar.

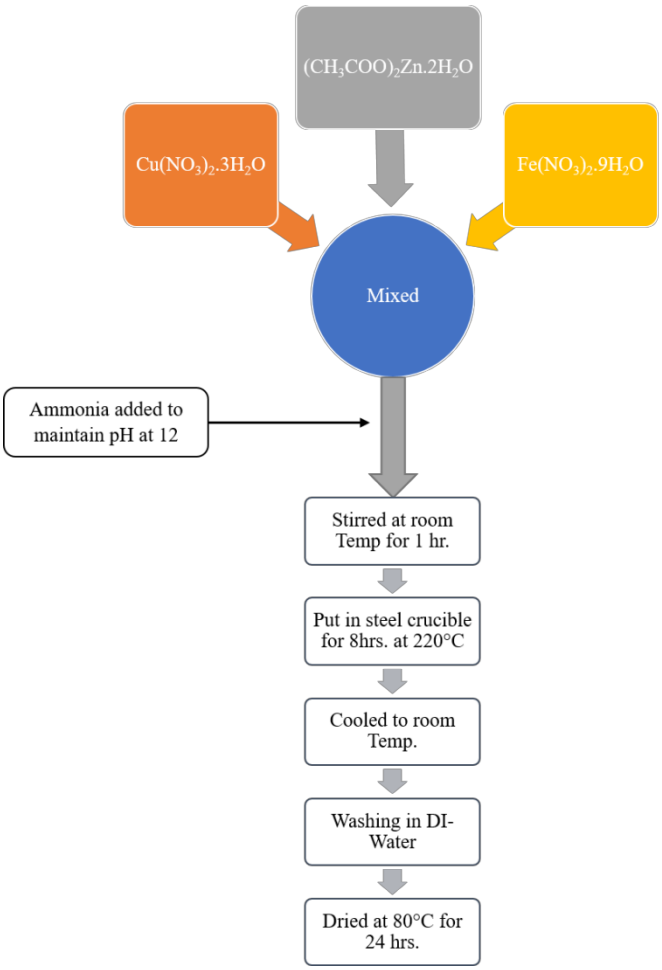

Fig. 2. Flow chart for preparation of Cu-Zn spinel ferrite through hydrothermal route

Characterization. Phase identification and structural characterization were performed using X-ray diffraction technique (Target: Cu-Kα, 10°-90°, step size – 0.02°, holding time: 0.2 seconds) which confirms the existence of a well-defined single-phase spinel ferrite structure. The SEM image for ferrite powder synthesized by each method was obtained using SEM machine. VSM was done to determine magnetic properties like saturation magnetization, remanence, and coercivity.

3. Results and Discussion

Structural Properties. The general formula for spinel ferrite synthesized is $Cu_{(1-x)}Zn_xFe_2O_4$. Spectra from XRD for x = 0.2-0.8 are shown in Fig. 3 and Fig. 4 were matched with the standard XRD pattern of Cu-Zn spinel ferrite, and it confirmed that single phase Cu-Zn spinel ferrite is formed for both methods. The most intense peaks in all specimens are (220), (311), (222), (400), (422), (333), and (440) are found to be well-matched with single-phase cubic spinel. The average crystallite size for all the samples was calculated using Debye Scherrer's formula with respect to the high-intensity peak plane (311). Debye Scherrer's formula can be expressed to calculate the crystallite size [17-18].

$$t = \frac{0.9\lambda}{BCos\theta_B}, \quad (2)$$

where t – crystallite size (Å), λ – wavelength of incident X-rays (Å), θ_B – Bragg's angle (degree), B – width of major peak at FWHM (radian).

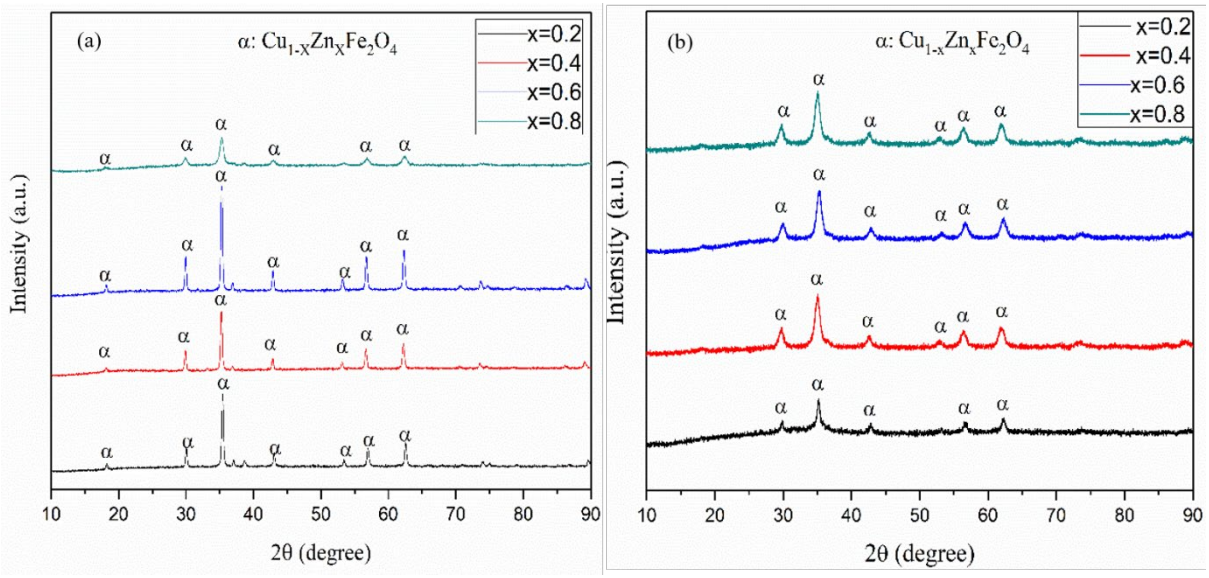

Fig. 3. XRD pattern for Cu-Zn spinel ferrite synthesized by (a) sol-gel auto-combustion method and (b) hydrothermal method

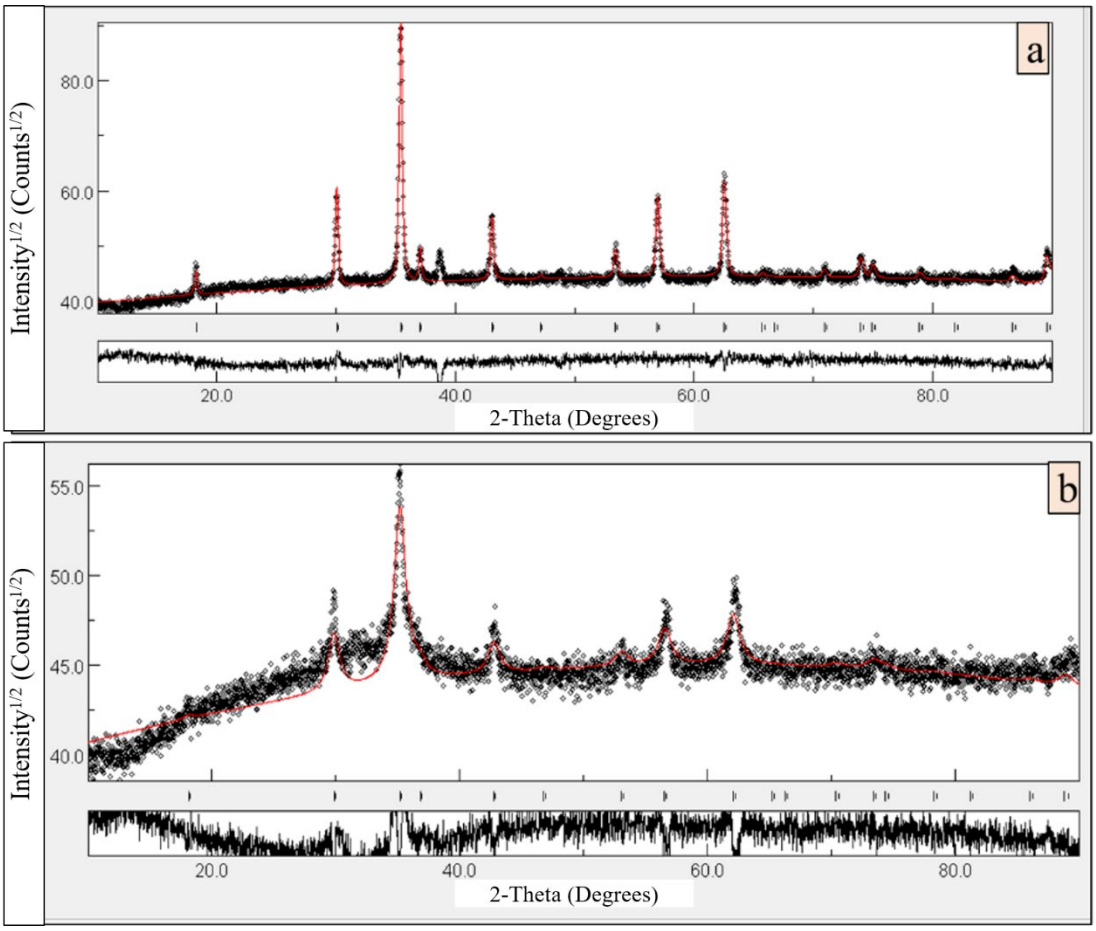

Fig. 4. Maud analysis of $Cu_{(1-x)}Zn_xFe_2O_4$ ferrite (a) Sol-gel (b) Hydrothermal

From Table 1 and Table 2, it can be noticed that the lattice parameter of Cu-Zn spinel ferrite increases with an increase in Zn substitution for both methods for x = 0.2–0.6. This can be explained as the size of the Zn ion is larger than the size of the Cu ion, so as we increase the concentration of Zn in the Cu-Zn spinel ferrite lattice parameter. But the value of the

lattice parameter decreases for x = 0.6–0.8, which can be explained as the further addition of Zn in the Cu-Zn spinel ferrite has led to a distortion of the lattice [19].

Table 1. Lattice parameter (a) and crystallite size (t) $Cu_{(1-x)}Zn_xFe_2O_4$ (x=0.2–0.8) ferrite nanopowders for sol-gel method

Sol-gel auto-combustion method		
x	**t (Å)**	**a (Å)**
0.2	764.098	8.3905
0.4	844.64	8.3974
0.6	657.11	8.4248
0.8	296.877	8.418

Table 2. Lattice parameter (a) and crystallite size (t) $Cu_{(1-x)}Zn_xFe_2O_4$ (x=0.2–0.8) ferrite nanopowders for hydrothermal method

Hydrothermal method		
x	**t (Å)**	**a (Å)**
0.2	296.877	8.418
0.4	302.687	8.423
0.6	205.465	8.472
0.8	175.317	8.4665

SEM. The SEM of Zinc doped copper ferrite is shown in Fig. 5. The image gives the impression that the product of the auto combustion reaction was very spongy and feathery, and it also confirms that the sub-micrometer-sized primary particles were agglomerated into the larger secondary particles. SEM has done for x=0.6 in $Cu_{(1-x)}Zn_xFe_2O_4$.

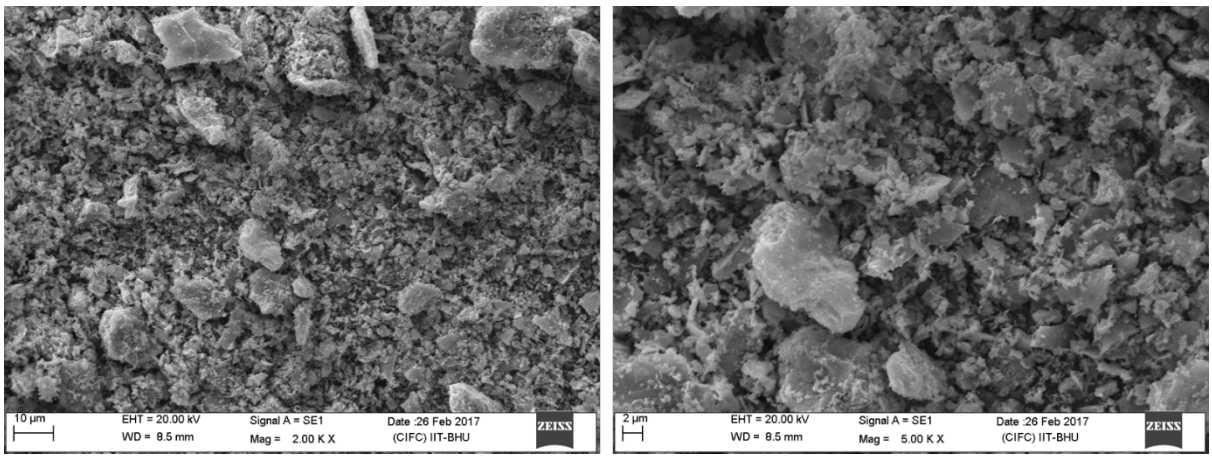

Fig. 5. SEM images of $Cu_{(1-X)}Zn_XFe_2O_4$ for x=0.6

Magnetic property. The saturation magnetization (Ms) and coercivity (Hc) of nanopowders synthesized by the sol-gel method as a function of Zn substitution (x) are shown in Fig. 6. It is observed that Ms gradually increases with an increase in Zn concentration for x=0.2–0.4 as the packing of magnetic material in a specified volume increases and then decreases with an increase in Zn concentration for x=0.6–0.8.

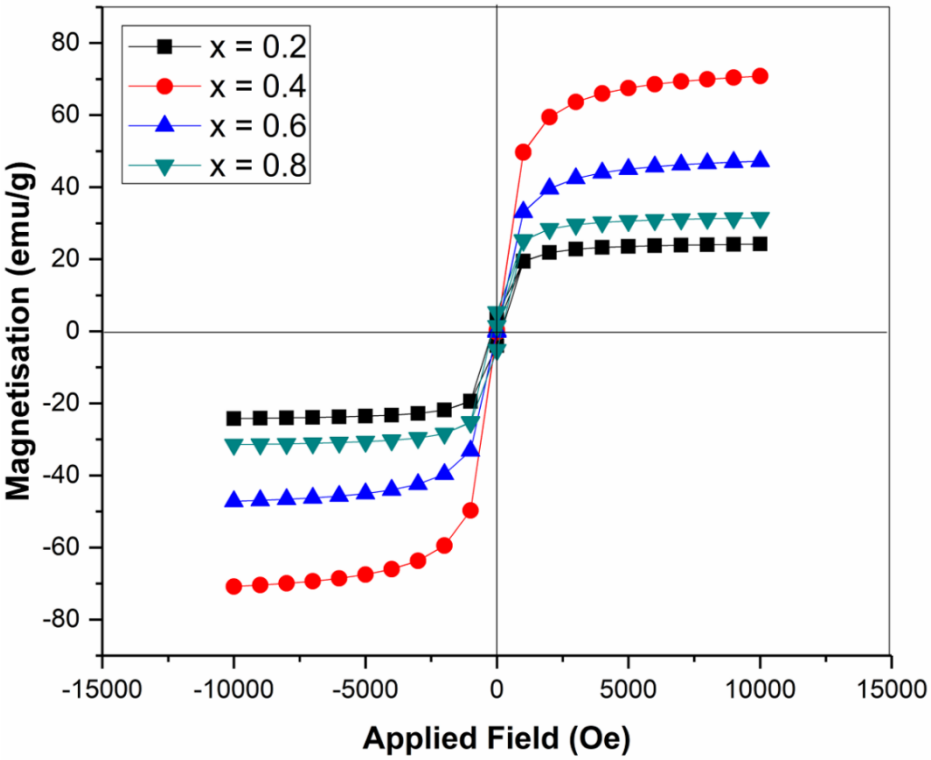

Fig. 6. Hysteresis loop for Cu-Zn spinel ferrite synthesized by sol-gel auto combustion method for varying composition of Zn (x)

Table 3. Values of Saturation magnetization (MS), Coercivity (H_C), and Remanence Magnetization (Mr)

Zn content	Ms (emu/g)	Mr (emu/g)	Hc (Oe)
x=0.2	24.21	6.14	184.47
x=0.4	70.82	5.33	174.46
x=0.6	47.21	3.22	116.26
x=0.8	31.17	2.33	102.26

The hysteresis plot of all synthesized samples shown in Fig. 6 and Table 3 enlists the effect of Zn doping on saturation magnetization (Ms), coercivity (Hc), and remenance (Mr). In the case of Zn Ferrite, the magnetic [20-22] properties can be explained by Neel's two sublattice models. According to this model, a spinel having a AB_2O_4 structure has two types of sublattices, octahedral (B) and tetrahedral (A) sites. Owing to exchange energy, the ions occupying A and B sites have their magnetic moments arranged in an anti-parallel fashion. Here, the Fe^{3+} ions are equally distributed amongst the A and B sites, while the Cu^{2+} ions have a strong preference for B sites. The net magnetic moment is determined by Cu^{2+} ($\mu B=1$) ions as the same due to Fe^{3+} ($\mu B=5$) ions present at A and B sites cancel out. Thus, the overall magnetization of the material is the difference in magnetization present at these two sites.
Site B dominates as it contains a more significant number of ions. However, on substituting Cu^{2+} with nonmagnetic ions Zn^{2+}. Zn^{2+} having a strong preference for A sites, they are disposed of there. This results in the dislocation of some of the Fe^{3+} ions from A to B sites. Unlike in the case of Cu ferrite, the compensation in the magnetic moment of Fe^{3+} will not occur, and they contribute with large magnetic moments to B sites. This results in an increase in magnetization. Mr and Hc present a decreasing nature with Zn doping. As seen, the minimum value of coercivity is obtained for x=0.8, with a general decreasing trend for

increasing x value. It is possibly due to the alternation of particle and grain size of Cu ferrite before and after Zn doping. Zn doped Cu ferrite, having a larger particle size, may have more magnetic domain and domain walls, resulting in demagnetization with ease. Also, the anisotropic constant value of Cu ferrite is more than that of Zn ferrite.

4. Conclusions

Cu-Zn spinel ferrite having chemical formula $Cu_{(1-x)}Zn_xFe_2O_4$was synthesized for x ranging from 0.2 to 0.8 by sol-gel auto-combustion method and hydrothermal method, and its single phase was verified by XRD results. An increasing trend in lattice parameter was observed for x=0.2-0.6 for both methods as the size of Zn ion is more than the size of Cu ion, and then it decreases for x=0.8 due to lattice distortion. From VSM results, it was observed that saturation magnetization increases as Zn doping increases from 0.2 to 0.4, i.e., 24.21 to 70.82 emu/g then Ms decreases with an increase in Zn doping from 47.21 to 31.17 for x= 0.6–0.8 as initially, Zn occupies A sites initially but with further increases in Zn doping causes saturation of Zn ions at A site and hence Zn ions to occupy B site. This causes a decrease in Ms with an increase in Zn doping. Mr and Hc decrease with an increase in Zn doping.

Acknowledgements. *No external funding was received for this study.*

References

[1] Li LZ, Peng L, Zhong XX, Wang R, Tu XQ. Structural, magnetic and electrical properties of Cu-Zn ferrite nanopowders. *Journal of Magnetism and Magnetic Materials*. 2016;419:407-411.

[2] Gao JM, Cheng F. Study on the preparation of spinel ferrites with enhanced magnetic properties using limonite laterite ore as raw materials. *Journal of Magnetism and Magnetic Materials*. 2018;460: 213-222.

[3] Mahmoud MH, Hassan AM, Said AE-AA, Hamdeh HH. Structural; magnetic and Catalytic properties of nanocrystalline $Cu_{0.5}Zn_{0.5}Fe_2O_4$ synthesized by microwave combustion and ball milling methods. *Journal of Molecular Structure*. 2016;1114: 1-6.

[4] Maria KH, Choudhury S, Hakim MA. Structural phase transformation and hysteresis behavior of Cu-Zn ferrites. *International Nano Letters*. 2013;3.

[5] Kavas H, Baykal A, Demir A, Toprak MS, Aktas B. $Zn_xCu_{(12x)}Fe_2O_4$ Nanoferrites by Sol–Gel Auto Combustion Route: Cation Distribution and Microwave Absorption Properties. *J. Inorg. Organomet. Polym*. 2014;24: 963-970.

[6] Wu W, Cai J, Wu X, Wang K, Hu Y, Wang Q. Nanocrystalline $Cu_{0.5}Zn_{0.5}Fe_2O_4$: Preparation and Kinetics of Thermal Decomposition of Precursor. *J. Supercond. Nov. Magn*. 2013;26: 3523-3528.

[7] Tatarchuk T, Bououdina M, Macyk W, Shyichuk O, Paliychuk N, Yaremiy I, Al-Najar B, Pacia M. Structural, Optical, and Magnetic Properties of Zn-Doped $CoFe_2O_4$ Nanoparticles. *Nanoscale Research Letters*. 2017;12.

[8] Yadav RS, Kuritka I, Havlica J, Hnatko M, Alexander C, Masilko J, Kalina L, Hajduchova M, Rusnak J, Enev V. Structural, Magnetic, Elastic, Dielectric and Electrical Properties of Hot-Press Sintered $Co_{1-x}Zn_xFe_2O_4$ (x=0.0, 0.5) Spinel Ferrite Nanoparticles. *Journal of Magnetism and Magnetic Materials*. 2017;447: 48-57.

[9] Parashar J, Saxena VK, Jyoti, Bhatnagar D, B.Sharma K. Dielectric behaviour of Zn substituted Cu nano-ferrites. *Journal of Magnetismand Magnetic Materials*. 2015;394: 105-110.

[10] Yadav RS, Havlica J, Hnatko M, Šajgalík P, Alexander C, Palou M, Bartonickova E, Bohac M, Frajkorova F, Masilko J, Zmrzly M, Kalina L, Hajdúchova M , Enev V. Magnetic properties of $Co_{1-x}Zn_xFe_2O_4$ spinel ferrite nanoparticles synthesized by starch-assisted sol–gel

autocombustion method and its ball milling. *Journal of Magnetism and Magnetic Materials*. 2015;378: 190-199.
[11] Baykal A, Esir S, Demir A, Güner S. Magnetic and optical Properties of $Cu_{1-x}Zn_xFe_2O_4$ Nanoparticles Dispersed in a silica matrix by a solgel auto-combustion method. *Ceramics International*. 2014;41(1): 231-239.
[12] Rana MU, Abbas T. The effect of Zn substitution on microstructure and magnetic properties of $Cu_{1-x}Zn_xFe_2O_4$ ferrite. *Journal of Magnetism and Magnetic Materials*. 2002;246(1-2): 110-114.
[13] Ajmal M, Maqsood A. Structural, electrical and magnetic properties of $Cu_{1-x}Zn_xFe_2O_4$ ferrites ($0 \leq x \leq 1$). *Journal of Alloys and Compounds*. 2008;460(1-2): 54-59.
[14] Hu J, Ma Y, Kan X, Liu C, Zhang X, Rao R, Wang M, Zheng G. Investigations of Co substitution on the structural and magnetic properties of Ni-Zn spinel ferrite. *Journal of Magnetism and Magnetic Materials*. 2020;513: 167200.
[15] Agarwal N, Narang SB. Magnetic characterization of Nickel-Zinc spinel ferrites along with their microwave characterization in Ku band. *Journal of Magnetism and Magnetic Materials*. 2020;513: 167052.
[16] Tangcharoen T, Ruangphanit A, Pecharapa W. Structural and magnetic properties of nanocrystalline zinc-doped metal ferrites (metal¼Ni; Mn;Cu) prepared by sol–gel combustion method. *Ceramics International*. 2013;39(S1): S239-S243.
[17] Nigam A, Pawar SJ. Structural, magnetic, and antimicrobial properties of zinc doped magnesium ferrite for drug delivery applications, *Ceramics International.* 2020;46: 4058-4064.
[18] Nigam A, Pawar SJ. Synthesis and characterization of ZnO nanoparticles to optimize drug loading and release profile for drug delivery applications. *Materials Today: Proceedings.* 2020;26(2): 2625-2628.
[19] Kumar N, Bharti A, Kumar A, Nigam A. Effect of process parameters on the crystal-parameters of Cu-Zn spinel-ferrites. *Materials Physics and Mechanics.* 2021;47: 65-73.
[20] Khudyakov A, Mazur A, Pleshakov I, Bibik E, Fofanov Y, Kuzmin Y, Shlyagin M. Transverse Relaxation of a Nuclear Spin System in Bulk and Nanostructured Magnetically Ordered Materials. In: *Proceedings of the 2020 IEEE International Conference on Electrical Engineering and Photonics.* EExPolytech; 2020. p.201-203.
[21] Esarev IV, Gurzhiy VV, Selyutin AA, Laptenkova AV, Poddel'skyc AI, Medvedskiy NL, Ponyaev AI, Trifonov RE, Eremin AV. First example of a click-reaction on the aminate copper complexes: effect of reaction parameters. *Mendeleev Communications.* 2018;28(6): 606-608.
[22] Singh S, Goswami G, Kumar A. Influence of Ph and Calcination Temperature on Magnetic Properties of Nanosized Zn-Ferrite Synthesized by Sol–Gel Citrate Method. *International Journal of Research in Engineering and Technology.* 2017;06(01): 23-29.